

10-63-CR
001
19671
p. 23

Progress Report

Submitted to: NASA Langley Research Center

Grant Title: ROBUST STABILITY OF SECOND-ORDER SYSTEMS

Grant Number: NAG-1-1397

Organization: Georgia Institute of Technology
Atlanta, GA 30332-0150

Principal Investigator: Dr. C.-H. Chuang
School of Aerospace Engineering
Georgia Institute of Technology
Atlanta, GA 30332-0150
(404) 894-3075

Period Covered: Aug. 24, 1993 to Aug. 24, 1994

Date of Submission: Aug. 19, 1994

(NASA-CR-196384) ROBUST STABILITY
OF SECOND-ORDER SYSTEMS Progress
Report, 24 Aug. 1993 - 24 Aug. 1994
(Georgia Inst. of Tech.) 23 p

N94-37590

Unclas

G3/63 0019671

Summary

This particular research project has a no cost extension until May 23, 1995. The extension is due to unexpected funding cut at the second year of this three years (proposed) project. This progress report gives current progress of the research in nonlinear robust control using positive real concept.

The progress is documented in the following draft paper. In the paper, the manipulator dynamics is reformulated differently from the existing equations of motion for free base robots. This new formulation gives a compact form of the dynamic equations for easy computation. The nonlinear terms are now considered. The results show that for an additional nonlinear friction term, the feedback controller designed using passivity concept works quite well. Although, design of such a controller requires simulation of the dynamics, for the example shown in the following draft, this design procedure is feasible.

NONLINEAR CONTROL OF SPACE MANIPULATORS WITH MODEL UNCERTAINTY

Manoj Mittal¹ and C. -H. Chuang²
School of Aerospace Engineering
Georgia Institute of Technology
Atlanta, Georgia 30332-0150

and

Jer-Nan Juang³
Spacecraft Dynamics Branch
NASA Langley Research Center
Hampton, Virginia

Abstract

Nonlinear control using feedback linearization or inverse dynamics for robotic manipulators yields good results in the absence of modeling uncertainty. However, modeling uncertainties due to unknown joint friction coefficients and payload variations can give rise to undesirable characteristics when these control systems are implemented. In this work, it is shown how passivity concepts can be used to supplement the feedback linearization control design technique, in order to make it robust with respect to the uncertain effects mentioned above. Results are obtained for space manipulators with freely floating base; however, they are applicable to fixed base manipulators as well. The controller guarantees asymptotic tracking of the joint variables. Closed-loop simulation results are illustrated for planar space manipulators for cases where uncertainty exists in friction modeling and payload inertial parameters.

1. Introduction

The dynamics of space manipulators differs from that of fixed base manipulators since their base is free to move. The base could be either a spacecraft or a satellite. The movement of manipulator arms produces reaction forces and torques on the base. Therefore the resulting motion of the base has to be accounted for in the dynamic model for the manipulator. However, Papadopoulos and Dubowsky¹ showed that a dynamic model for space manipulators with a free base is similar in structure to the dynamic model for fixed base manipulators. An obvious

¹Postdoctoral Fellow

²Assistant Professor

³Principal Scientist

similarity is that the inertia matrix in each case is symmetric and positive definite. In fact, the dynamic model for fixed base manipulators can be viewed as forming a subset of that for space manipulators.

Some concepts have been proposed for joint trajectory control and inertial end tip motion control of space manipulators. Vafa and Dubowsky² developed an analytical tool for space manipulators, known as the virtual manipulator concept. The virtual manipulator is an idealized kinematic chain connecting its base, the virtual base, to any point on the real manipulator. This point can be chosen to be the manipulator's end effector, while the virtual base is located at the system center of mass, which is fixed in inertial space. As the real manipulator moves, the end of the virtual manipulator remains coincident with the selected point on the real manipulator. Additionally, it can be shown that the change in orientation in the virtual manipulator's joints is equal to the change in the orientation of the real manipulator's joints. While these features give the designer the ability to represent a free floating space manipulator by a simpler system whose base is fixed in inertial space, the associated transformation depends on knowing the system parameters exactly. Alexander and Cannon³ showed that the end tip of the space robot can be controlled by solving the inverse dynamics that includes motion of the base. Their method assumes the mass of the spacecraft to be relatively large compared to that of the manipulator it carries, and also requires much computational effort to determine the control input. Note that some future space systems are expected to have the manipulator and spacecraft masses of the same order. Umetani and Yoshida⁴ proposed the generalized Jacobian matrix that relates the end tip velocities to the joint velocities by taking into account the motion of the base. However, robustness of the control scheme with respect to modeling uncertainties is not discussed. Masutani et. al.⁵ proposed a sensory feedback control scheme based on an artificial potential defined in the sensor coordinate frame. This scheme is based on proportional feedback of errors in the end tip position and orientation as well as feedback of joint angular velocities. A robust controller based on feedback linearization using a simplified nonlinear model and passivity concepts was developed by Chuang, Mittal, and Juang⁶.

In this paper a robust control scheme using feedback linearization of the complete model and passivity concepts is proposed for space manipulators in which joint friction and mass variations are considered. The proposed technique can be used for fixed base manipulators also. The control scheme uses inverse dynamics; however, it is robust in the face of bounded modeling uncertainties which might arise due to improper or absent friction modeling as well as payload variations. The controller asymptotically tracks prescribed time varying joint angle trajectories whose acceleration is bounded in the L^2 space. Although only two types of uncertain dynamic effects are considered here, the controller can be applied to systems with other types of uncertainty.

2. Dynamics of Space Manipulator System with Uncontrolled Base

This development of a nonlinear dynamical model for space manipulator systems whose base is uncontrolled is discussed in this Section. The development of the expressions for linear and angular momenta of the system closely follows that given in Reference [5], however, the form of the final equations of motion is different. A space manipulator system in the satellite orbit can be approximately considered to be floating in a non-gravitational environment. As shown in Figure 1, the manipulator and the base can be treated as a set of $n+1$ rigid bodies connected through n joints. The bodies are numbered from zero to n with the base being 0 and the end tip being n . Each joint is then numbered accordingly from one to n . The angular displacements of the joints can be represented by a joint vector,

$$\mathbf{q} = [q_1 \ q_2 \ \dots \ q_n]^T \quad (1)$$

The mass and inertia tensor of the i^{th} body are denoted by m_i and I_i ; and the inertia tensor is expressed in terms of the base frame coordinates.

2.1 Kinematics

A coordinate frame fixed to the orbit of the satellite can be considered to be an inertial frame, denoted by Σ_I . In addition to Σ_I , another coordinate frame Σ_B is defined that is attached to the base with its origin located at the base center of mass. The attitude of the base itself is given by roll, pitch, and yaw angles. In the sequel, all vectors are expressed in the base fixed coordinate axes.

Let R_i and r_i be the position vectors of the center of mass of the i^{th} link with respect to frames Σ_I and Σ_B , respectively. Then

$$R_i = R_B + r_i \quad (2)$$

where R_B is the position vector from the base center of mass to the origin of the frame Σ_I . Let V_i and Ω_i be the linear and angular velocities of the center of mass of the i^{th} link with respect to frame Σ_I and v_i and ω_i be the linear and angular velocities of the same point with respect to frame Σ_B . Then V_i and Ω_i can be written as

$$V_i = V_B + v_i + \Omega_B \times r_i \quad (3)$$

$$\Omega_i = \Omega_B + \omega_i \quad (4)$$

V_B and Ω_B are the linear and angular velocities of the base center of mass with respect to frame Σ_I . Note that for any space manipulator, v_i and ω_i for each link can be represented by the following forms

$$v_i = J_{L_i}(q)\dot{q} \quad (5)$$

$$\omega_i = J_{A_i}(q)\dot{q} \quad (6)$$

where $J_{L_i}(q)$ and $J_{A_i}(q) \in \mathbb{R}^{3 \times n}$ are the Jacobian matrices for the i^{th} link.

The position of the system center of mass with respect to the base frame depends on the joint angles. Given below are two measures related to the system center of mass.

$$m_c = \sum_{i=0}^n m_i \quad (7)$$

$$r_c(q) = \frac{\sum_{i=0}^n m_i r_i(q)}{m_c} \quad (8)$$

2.2 Linear and Angular Momenta

The linear momentum P and the angular momentum L of the whole system are defined as follows

$$P = \sum_{i=0}^n m_i V_i \quad (9)$$

$$L = \sum_{i=0}^n [I_i \Omega_i + m_i R_i \times V_i] \quad (10)$$

Substituting Equations (2) through (8) into Equations (9) and (10) yields

$$P = H_v V_B + H_{v\Omega} \Omega_B + H_{vq} \dot{q} \quad (11)$$

$$L = H_{v\Omega}^T V_B + H_{\Omega} \Omega_B + H_{\Omega q} \dot{q} + R_B \times P \quad (12)$$

where

$$H_v = m_c I, \quad H_v \in \mathbb{R}^{3 \times 3} \quad (13)$$

$$H_{v\Omega} = -m_c [r_c \times], \quad H_{v\Omega} \in \mathbb{R}^{3 \times 3} \quad (14)$$

$$H_{vq} = \sum_{i=1}^n m_i J_{L_i}, \quad H_{vq} \in \mathbb{R}^{3 \times n} \quad (15)$$

$$H_{\Omega} = \sum_{i=0}^n I_i + \sum_{i=1}^n m_i [r_i \times]^T [r_i \times], \quad H_{\Omega} \in \mathbb{R}^{3 \times 3} \quad (16)$$

$$H_{\Omega q} = \sum_{i=1}^n \{I_i J_{A_i} + m_i [r_i \times] J_{L_i}\}, \quad H_{\Omega q} \in \mathbb{R}^{3 \times n} \quad (17)$$

Also, for any vector

$$f = \begin{bmatrix} f_1 \\ f_2 \\ f_3 \end{bmatrix}, \quad (18)$$

$[f \times]$ is defined as follows

$$[f \times] \equiv \begin{bmatrix} 0 & -f_3 & f_2 \\ f_3 & 0 & -f_1 \\ -f_2 & f_1 & 0 \end{bmatrix} \quad (19)$$

and I is an identity matrix of appropriate dimensions.

Since the working environment is non-gravitational and no actuators generating external forces are employed, the linear and angular momenta of the whole system are conserved. Since the inertial frame is fixed to the orbit, the whole system can be assumed to be stationary with respect to the inertial frame at the initial state. Thus the above two momenta are always zero for the whole system. Note that it is implicitly implied that the satellite is a non-spinning body. By using the fact then that the linear and angular momenta are zero, Equations (11) and (12) result in

$$V_B = -H_v^{-1} [H_{v\Omega} \Omega_B + H_{vq} \dot{q}] \quad (20)$$

$$\Omega_B = -[H_{\Omega} - H_{v\Omega}^T H_v^{-1} H_{v\Omega}]^{-1} [H_{\Omega q} - H_{v\Omega}^T H_v^{-1} H_{vq}] \dot{q} \quad (21)$$

2.3 Manipulator Dynamics

The total kinetic energy of the space robot can be written as

$$T = \frac{1}{2} \sum_{i=0}^n (m_i V_i^T V_i + \Omega_i^T I_i \Omega_i) \quad (22)$$

Using Equations (3) through (8) and (13) through (17) the kinetic energy can be expressed as

$$T = \frac{1}{2} \begin{bmatrix} \mathbf{V}_B^T & \boldsymbol{\Omega}_B^T & \dot{\mathbf{q}}^T \end{bmatrix} \begin{bmatrix} H_v & H_{v\Omega} & H_{vq} \\ H_{v\Omega}^T & H_\Omega & H_{\Omega q} \\ H_{vq}^T & H_{\Omega q}^T & H_q \end{bmatrix} \begin{bmatrix} \mathbf{V}_B \\ \boldsymbol{\Omega}_B \\ \dot{\mathbf{q}} \end{bmatrix} \quad (23)$$

where H_q is the inertia matrix corresponding to the fixed base manipulator

$$H_q = \sum_{i=1}^n [m_i J_{Li}^T J_{Li} + J_{Ai}^T I_i J_{Ai}], \quad H_q \in \mathbb{R}^{n \times n} \quad (24)$$

Equation (23) for the system kinetic energy can be simplified as follows. Substituting for \mathbf{V}_B from Equation (20) leads to

$$T = \frac{1}{2} \boldsymbol{\Omega}_B^T \mathbf{M} \boldsymbol{\Omega}_B + \boldsymbol{\Omega}_B^T \mathbf{Z} \dot{\mathbf{q}} + \frac{1}{2} \dot{\mathbf{q}}^T \mathbf{W} \dot{\mathbf{q}} \quad (25)$$

where

$$\mathbf{M} = H_\Omega - H_{v\Omega}^T H_v^{-1} H_{v\Omega}, \quad \mathbf{M} \in \mathbb{R}^{3 \times 3} \quad (26)$$

$$\mathbf{Z} = H_{\Omega q} - H_{v\Omega}^T H_v^{-1} H_{vq}, \quad \mathbf{Z} \in \mathbb{R}^{3 \times n} \quad (27)$$

$$\mathbf{W} = H_q - H_{vq}^T H_v^{-1} H_{vq}, \quad \mathbf{W} \in \mathbb{R}^{n \times n} \quad (28)$$

Further, substituting for $\boldsymbol{\Omega}_B$ from Equation (21), one obtains an expression for the system kinetic energy solely in terms of the joint variables

$$T = \frac{1}{2} \dot{\mathbf{q}}^T \mathbf{D}(\mathbf{q}) \dot{\mathbf{q}}, \quad \mathbf{D} \in \mathbb{R}^{n \times n} \quad (29)$$

where \mathbf{D} is the inertia matrix of the system and is given by

$$\mathbf{D} = \mathbf{W} - \mathbf{Z}^T \mathbf{M}^{-1} \mathbf{Z} \quad (30)$$

It can be shown that $\mathbf{D} = \mathbf{D}^T > 0$. It is interesting to note that the system inertia matrix obtained in Reference [1] is of the same form as the above. However, the expressions for \mathbf{W} , \mathbf{M} , and \mathbf{Z} matrices are different. This is because a different approach, viz. the concept of barycenters, is used in the model derivation of Reference [1].

Since there is no potential energy in non-gravitational environment, the Lagrangian Λ , is equal to the kinetic energy

$$\Lambda = T \quad (31)$$

So the system dynamics is given by

$$\frac{d}{dt} \left(\frac{\partial \Lambda}{\partial \dot{q}} \right) - \frac{\partial \Lambda}{\partial q} = \tau \quad (32)$$

where τ is an $n \times 1$ vector of joint torques. The equations of motion for space manipulators can then be written as

$$D(q)\ddot{q} + h(q, \dot{q}) = \tau \quad (33)$$

where

$$h(q, \dot{q}) = C(q, \dot{q})\dot{q} + \tau_f \quad (34)$$

Paralleling the development for fixed base robots given by Spong and Vidyasagar⁷, the elements of the matrix C are obtained as

$$C_{kj} = \frac{1}{2} \sum_{i=1}^n \left[\frac{\partial D_{kj}}{\partial q_i} + \frac{\partial D_{ki}}{\partial q_j} - \frac{\partial D_{ij}}{\partial q_k} \right] \dot{q}_i \quad (35)$$

and τ_f represents the joint torque vector due to friction. As pointed out by Craig⁸, the total friction at each joint can be taken to be the sum of Coulomb friction and viscous friction. Coulomb friction is constant except for a sign dependence on the joint velocity. Viscous friction, in general, depends on various powers of joint velocity. However, higher powers contribute significantly only at high joint velocities. Manipulators usually do not attain such high velocities. Therefore, it is sufficient to consider only the linear dependence of viscous friction on joint velocity. Figure 2 shows a friction model consisting of Coulomb friction and linear viscous friction. Using this model, the joint friction torque vector can be represented as

$$\tau_f = \Psi \text{sgn}(\dot{q}) + \Gamma \dot{q} \quad (36)$$

where Ψ is a diagonal matrix consisting of Coulomb friction constants for the joints, and Γ is a diagonal matrix consisting of viscous friction coefficients for the manipulator joints. It turns out that in many manipulator joints, friction also displays a dependence on joint position. However, such effects are not considered here. There are other effects like bending effects that are difficult to model and also neglected in the present model.

2.4 Base Motion

The translational velocity of the base center of mass can be written in terms of joint velocities by using the expression for Ω_B from Equation (21) in Equation (20).

$$\mathbf{V}_B = -\mathbf{H}_v^{-1}[\mathbf{H}_{vq} - \mathbf{H}_{v\Omega}\mathbf{M}^{-1}\mathbf{Z}]\dot{\mathbf{q}} \quad (37)$$

Also, the base angular velocity from Equation (21) is

$$\Omega_B = -\mathbf{M}^{-1}\mathbf{Z}\dot{\mathbf{q}} \quad (38)$$

Using the above expressions, the evolution of the base position and orientation with time can be determined as follows

$$\begin{bmatrix} \dot{x}_b \\ \dot{y}_b \\ \dot{z}_b \end{bmatrix} = \begin{bmatrix} c_\psi c_\theta & c_\psi s_\theta s_\phi - s_\psi c_\phi & c_\psi s_\theta c_\phi + s_\psi s_\phi \\ s_\psi c_\theta & s_\psi s_\theta s_\phi + c_\psi c_\phi & s_\psi s_\theta c_\phi - c_\psi s_\phi \\ -s_\theta & c_\theta s_\phi & c_\theta c_\phi \end{bmatrix} \mathbf{V}_B \quad (39)$$

$$\begin{bmatrix} \dot{\phi} \\ \dot{\theta} \\ \dot{\psi} \end{bmatrix} = \begin{bmatrix} 1 & s_\phi \tan(\theta) & c_\phi \tan(\theta) \\ 0 & c_\phi & -s_\phi \\ 0 & s_\phi \sec(\theta) & c_\phi \sec(\theta) \end{bmatrix} \Omega_B \quad (40)$$

where $c_{(\cdot)} \equiv \cos(\cdot)$, $s_{(\cdot)} \equiv \sin(\cdot)$.

3. Control System Design

Assuming that the dynamics of the space manipulator is described by Equation (33), where \mathbf{D} and \mathbf{h} are completely known, the feedback linearization or inverse dynamics⁷ technique can be used to design controllers for tracking prescribed command trajectories for the joint angles. This can be accomplished as outlined in the following sub-section.

3.1 Feedback Linearization

Let the joint torque vector be of the following form.

$$\tau = Du + h \quad (41)$$

where u is the pseudo-control, i.e., it is the control input to the resulting linearized system. With the control law given by Equation (41), the closed-loop system becomes

$$\begin{bmatrix} \dot{q} \\ \ddot{q} \end{bmatrix} = A \begin{bmatrix} q \\ \dot{q} \end{bmatrix} + Bu \quad (42)$$

where

$$A = \begin{bmatrix} 0 & I \\ 0 & 0 \end{bmatrix}, B = \begin{bmatrix} 0 \\ I \end{bmatrix} \quad (43)$$

A simple PD (Proportional-Derivative) type of control law is chosen for the feedback linearized system

$$u = \ddot{q}_d + K_2(\dot{q}_d - \dot{q}) + K_1(q_d - q) \quad (44)$$

where K_1 and K_2 are proportional and derivative gain matrices, respectively. These matrices are usually chosen to be diagonal in order to achieve decoupled response among the joint angles. Substituting for u from Equation (44) into Equation (42), one obtains

$$\dot{e} = A_c e \quad (45)$$

where $e = [e_1^T \ e_2^T]^T$, $e_1 = q_d - q$, $e_2 = \dot{q}_d - \dot{q}$, $A_c = A - BK$, and $K = [K_1 \ K_2]$. If $K_1 > 0$ and $K_2 > 0$, the error dynamics as given by Equation (45) is asymptotically stable. The freedom in selecting the gain matrices can be utilized to meet performance specifications for the closed-loop system.

The preceding discussion assumes availability of perfect knowledge about the nonlinear system dynamics. However, in practice, D and h are usually imprecisely known due to modeling inaccuracies. It is assumed that the controller is designed using best estimates for friction models and for a nominal value of the end-tip payload. The actual joint friction will be different from that assumed in controller design, and the actual tasks might require handling a variety of payloads. Thus the controller uses computed versions of D and h . The objective here is to design a control law that is robust for bounded variations in D and h due to the uncertain dynamic effects in friction

and payload. This issue of robust control design is discussed in the following sub-section, where it will be seen that the control law results in closed-loop asymptotic tracking.

3.2 Robust Feedback Linearization Using Passivity

In the presence of modeling uncertainties, the control law is given as

$$\tau = D_c u + h_c \quad (46)$$

where D_c and h_c are computed versions of D and h respectively. Substituting for τ and u from Equations (46) and (44) into Equation (33) it can be shown that the closed-loop system dynamics is given by

$$\dot{e} = A_c e + Bv \quad (47)$$

where

$$v = \Delta u + \delta \quad (48)$$

and

$$\Delta = [I - D^{-1}D_c], \quad \delta = D^{-1}[h - h_c] \quad (49)$$

The first step in the proposed design is to choose the gain matrix $K = [K_1 \ K_2]$ and an output matrix F such that the linear system given by

$$\begin{aligned} \dot{e} &= A_c e + Bv \\ y &= Fe \end{aligned} \quad (50)$$

is SPR (Strictly Positive Real). This can be achieved as outlined in the following theorem. A definition of the concept of Strictly Positive Realness can be found in Slotine and Li⁹.

Theorem 1 [10]. Let K_1 and K_2 be such that

$$\begin{aligned}
K_1 &= \text{diag}[k_{1i}]; \quad k_{1i} > 0, \quad i = 1, \dots, n \\
K_2 &= \text{diag}[k_{2i}]; \quad k_{2i} > 0, \quad i = 1, \dots, n \\
(k_{2i})^2 &> k_{1i}, \quad i = 1, \dots, n
\end{aligned} \tag{51}$$

then if $F = K$, the system described by Equation (50) is SPR.

Note that the conditions of the Theorem as prescribed by (51) are extremely easy to satisfy.

With the linear System (50) being SPR, the Passivity Theorem¹¹ can be used to design asymptotically stable controllers as shown in the following theorem. The notation $\|x\|_T = \left(\int_0^T x^T x \, dt \right)^{1/2}$ is used in the sequel.

Theorem 2. Let the desired trajectory for joint variables be such that $\ddot{q}_d \in L^2$. Further, in the control law given by Equation (46), let h_c be such that

$$\|D^{-1}[h - h_c]\|_T \leq c\|u\|_T + d \quad \forall T > 0 \quad (c \geq 0, \infty > d \geq 0) \tag{52}$$

If D_c is chosen such that

$$D^{-1}D_c \geq arI \quad (a > 0, r > 0) \tag{53}$$

where

$$a > \frac{c+1}{r} \tag{54}$$

then the closed-loop System (47) is asymptotically stable.

Proof. The closed-loop system as given by Equation (47) can be represented in block diagram form as shown in Figure 3. It is first shown that the nonlinear block in the feedback path is passive¹¹. Consider

$$\begin{aligned}
I &= \int_0^T -u^T v \, dt \quad (T > 0) \\
&= \int_0^T -u^T (\Delta u + \delta) \, dt
\end{aligned}$$

$$= \left(-\int_0^T u^T \Delta u dt \right) + \left(-\int_0^T u^T \delta dt \right) \quad (55)$$

Let the first and second integrals on the right hand side be denoted by I_1 and I_2 respectively. Then

$$I_1 = \int_0^T u^T [D^{-1}D_c - I] u dt \quad (56)$$

Noting that Inequality (53) gives rise to $D^{-1}D_c - I \geq (ar - 1)I$, Equation (56) can be used to obtain the following.

$$I_1 \geq (ar - 1) \|u\|_T^2 \quad (57)$$

On the other hand,

$$\begin{aligned} -I_2 &= \int_0^T u^T D^{-1} [h - h_c] dt \\ &\leq \|u\|_T \|D^{-1} [h - h_c]\|_T \quad (\text{Hölder's Inequality}) \\ &\leq \|u\|_T [c \|u\|_T + d] \quad (\text{Inequality (52)}) \end{aligned} \quad (58)$$

Hence

$$I \geq (ar - c - 1) \|u\|_T^2 - d \|u\|_T = f(\|u\|_T) \quad (59)$$

It can be shown that if $(ar - c - 1) > 0$, then

$$f(\|u\|_T) \geq -\frac{d^2}{4(ar - c - 1)} \quad \forall \|u\|_T \geq 0 \quad (60)$$

which in turn would imply

$$\int_0^T -u^T v dt \geq -\frac{d^2}{4(ar - c - 1)} \quad \forall T > 0 \quad (61)$$

Thus a sufficient condition for the nonlinear block to be passive is that $a > (c + 1)/r$.

Additionally, the transfer function of the feedforward block $[A_c, B, K]$ is proper and has no poles on the imaginary axis. Hence it has finite gain¹². Since $\ddot{q}_d \in L^2$, then using the Passivity Theorem¹¹, one can conclude

that the signals u , Ke , and v are bounded. Moreover, since the feedforward block is SPR, $Ke(t) = K_1e_1(t) + K_2e_2(t)$ goes to zero asymptotically. This in turn implies that $e_1(t)$ and $e_2(t)$ individually approach zero asymptotically⁸.

Remark. The conventional method of designing robust controllers for robotics problems involves introducing an outer loop control⁷ in order to compensate for the uncertain dynamic effects. This has been known to introduce chattering in the control. When the design method is modified to make the control smooth, closed-loop asymptotic tracking is generally compromised to some extent. In the method proposed in Theorem 2, an outer loop control is not employed. Instead, achievement of robustness can be qualitatively understood as follows. Depending on the amount of uncertainty contained in h , the computed version of the inertia matrix D , is modified such that conditions (53) and (54) of the Theorem are satisfied.

The results of the Theorem are applicable to space manipulators as well as fixed base manipulators. Finally, it should be noted that the control design obtained using the results of the theorem is not unique. Additionally, there is a considerable amount of margin for performance optimization.

4. Simulation Results

As an example, results of applying Theorems 1 and 2 in order to achieve a robust control design will be illustrated for planar space robots. Nonlinear dynamic models for the robots are obtained using the results of Section 2. The controller is designed for nominal values of joint friction coefficients and payload mass; whereas the actual robot will be considered to have variations in these. Simulation is carried out using variable-step fourth and fifth-order Runge-Kutta methods. The base and link masses in the following examples are assumed to be of the same order of magnitude. Closed-loop results are generated for step command to the joint angles. Note that in general, for end tip motion control in the inertial space, the inverse kinematics problem needs to be solved in order to generate a command trajectory for the joint angle vector.

4.1 Planar One Link Space Manipulator

Figure 4 shows a planar one link space robot. Equation (33) describes the dynamics of this one degree of freedom system. The system inertia, computed using Equation (30), turns out to be

$$D(q_1) = W_{1,1} - Z_{3,1}^2 / M_{3,3} \quad (66)$$

where

$$W_{1,1} = m_{01}p_1^2 + I_1 \quad (67)$$

$$Z_{3,1} = m_{01}p_1(p_0c_1 + p_1) + I_1 \quad (68)$$

$$M_{3,3} = m_{01}(p_0^2 + p_1^2 + 2p_0p_1c_1) + I_0 + I_1 \quad (69)$$

Using Equations (34) and (35), h is determined to be

$$h(q_1, \dot{q}_1) = \frac{m_{01}p_0p_1s_1}{M_{3,3}^2} [m_{01}p_0(p_0 + p_1c_1) + I_0] \cdot [m_{01}p_1(p_0c_1 + p_1) + I_1] \dot{q}_1^2 + \psi \text{sgn}(\dot{q}_1) + \gamma \dot{q}_1 \quad (70)$$

where ψ and γ are respectively the coefficients of Coulomb and viscous friction. In Equations (67) through (70) $m_{01} = m_0m_1 / m_c$, $m_c = m_0 + m_1$, $c_1 \equiv \cos(q_1)$, and $s_1 \equiv \sin(q_1)$. The quantities m_1 , I_1 , and p_1 are defined for an "equivalent" link that is obtained by removal of the end tip payload and absorbing its inertial characteristics in those of the link itself. The concept of the equivalent link is explained in the Appendix.

It can be seen easily that as $m_0 \rightarrow \infty$ and $I_0 \rightarrow \infty$,

$$D \rightarrow m_1p_1^2 + I_1, \quad h \rightarrow \psi \text{sgn}(\dot{q}_1) + \gamma \dot{q}_1 \quad (71)$$

which represents the case of a fixed base manipulator. Equation (39) is used to determine the evolution of the base position with time

$$\begin{aligned} \dot{x}_b &= \frac{m_1}{m_c} \left[p_1s_{\psi 1} - \frac{Z_{3,1}}{M_{3,3}} (p_0s_{\psi} + p_1s_{\psi 1}) \right] \dot{q}_1 \\ \dot{y}_b &= \frac{m_1}{m_c} \left[-p_1c_{\psi 1} + \frac{Z_{3,1}}{M_{3,3}} (p_0c_{\psi} + p_1c_{\psi 1}) \right] \dot{q}_1 \end{aligned} \quad (72)$$

where $s_{\psi 1} \equiv \sin(\psi + q_1)$, $c_{\psi 1} \equiv \cos(\psi + q_1)$. Finally, the base attitude dynamics is obtained using Equation (40)

$$\dot{\psi} = -\frac{Z_{3,1}}{M_{3,3}} \dot{q}_1 \quad (73)$$

Next, a feedback controller is designed for the one link space manipulator using the results of Theorems 1 and 2. D_c and h_c are obtained from Equations (66) and (70) respectively, by using the nominal values of end-link parameters and friction coefficients:

$$D_c = D|_{m_1 \rightarrow m_{1c}, p_1 \rightarrow p_{1c}, I_1 \rightarrow I_{1c}} \quad (74)$$

$$h_c = h|_{m_1 \rightarrow m_{1c}, p_1 \rightarrow p_{1c}, I_1 \rightarrow I_{1c}, \psi \rightarrow \psi_c, \gamma \rightarrow \gamma_c}$$

Closed-loop results are generated for a step command of 1 radian to the joint angle. Table I lists physical parameters of the example robot used in simulation. The feedback gains are chosen to be $k_1 = 0.4$ and $k_2 = 1.0$. This choice of gains satisfies Conditions (51) and in case of no modeling uncertainty, yields a closed-loop response without any overshoot. Simulation results will be shown for the case in which there is no modeling uncertainty, and for another case that involves uncertainty.

Figures 5 through 8 show closed-loop responses for the nominal case. Figure 5 shows that asymptotic tracking in the joint angle is achieved. Figures 7 and 8 show that the base moves in reaction to link motion; this is due to the conservation of linear and angular momenta as discussed in Section 2. However, the joint angle still achieves the appropriate commanded value. The closed-loop responses for the case involving uncertainty will be overlaid on Figures 5 through 8.

5. Conclusions

A robust control method based on feedback linearization and passivity concepts is proposed for space manipulators. The method is applicable to fixed base manipulators as well. The control law results in asymptotic joint angle tracking in the face of bounded uncertainties in friction modeling and payload inertial characteristics. For the first time, closed-loop simulation results will be presented using this control method.

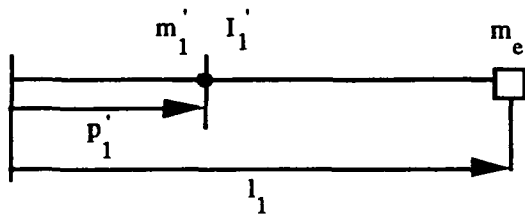
References

- [1]. E. Papadopoulos and S. Dubowsky, "On the Nature of Control Algorithms for Space Manipulators," Proceedings of the IEEE International Conference on Robotics and Automation, Cincinnati, Ohio, May 1990, pp. 1102-1108.
- [2]. Z. Vafa and S. Dubowsky, "The Kinematics and Dynamics of Space Manipulators: The Virtual Manipulator Approach," *The International Journal of Robotics Research*, Vol. 9, No. 4, August 1990, pp. 3-21.
- [3]. H. L. Alexander and R.H. Cannon, "Experiments on the Control of a Satellite Manipulator," Proceedings of the American Control Conference, Minneapolis, Minnesota, June 1987.

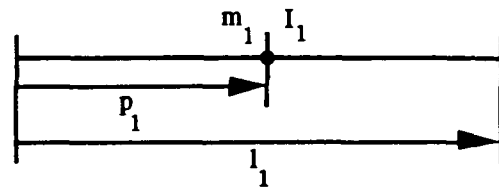
- [4]. K. Yoshida and Y. Umetani, "Control of Space Manipulators with Generalized Jacobian Matrix," in *Space Robotics: Dynamics and Control*, Eds. Y. Xu and T. Kanade, Kluwer Academic Publishers, Boston, Massachusetts, 1993, pp. 165-204.
- [5]. Y. Masutani, F. Miyazaki, and S. Arimoto, "Sensory Feedback Control For Space Manipulators," Proceedings of the 1989 IEEE International Conference on Robotics and Automation, Scottsdale, Arizona, May 1989, pp. 1346-1351.
- [6]. C. -H. Chuang, M. Mittal, and J. -N. Juang, "Passivity Based Robust Control of Space Manipulators," Proceedings of the AIAA Guidance, Navigation, and Control Conference, Monterey, California, August 1993.
- [7]. M. W. Spong and M. Vidyasagar, *Robot Dynamics and Control*, John Wiley, New York, 1989.
- [8]. J. J. Craig, *Introduction to Robotics Mechanics and Control*, Second Edition, Addison-Wesley, 1989, pp. 214-215.
- [9]. J-J. E. Slotine and W. Li, *Applied Nonlinear Control*, Prentice Hall, New Jersey, 1991, pp. 127, 399.
- [10]. C. Abdallah and R. Jordan, "A Positive-Real Design for Robotic Manipulators," Proceedings of the 1990 American Control Conference, San Diego, California, May 1990, pp. 991-992.
- [11]. C. A. Desoer and M. Vidyasagar, *Feedback Systems: Input-Output Properties*, Academic Press, New York, 1975, pp. 173-186.
- [11]. J. C. Doyle, B. A. Francis, and A. R. Tannenbaum, *Feedback Control Theory*, Macmillan, New York, 1992, pp. 16.

Appendix

The concept of an equivalent link is described here. Following are two equivalent representations of the same link. The Figure on the left shows the actual link, while the one on the right shows a hypothetical equivalent link that is obtained by removal of the end tip payload and absorbing its inertial characteristics into the link.



Actual Link



Equivalent Link

The geometric and mass properties of the equivalent link are given as follows:

$$m_1 = m_1 + m_e$$

$$p_1 = \frac{m_1 p_1 + m_e l_1}{m_1 + m_e}$$

$$I_1 = I_1 + \frac{m_1 m_e}{m_1 + m_e} (l_1 - p_1)^2$$

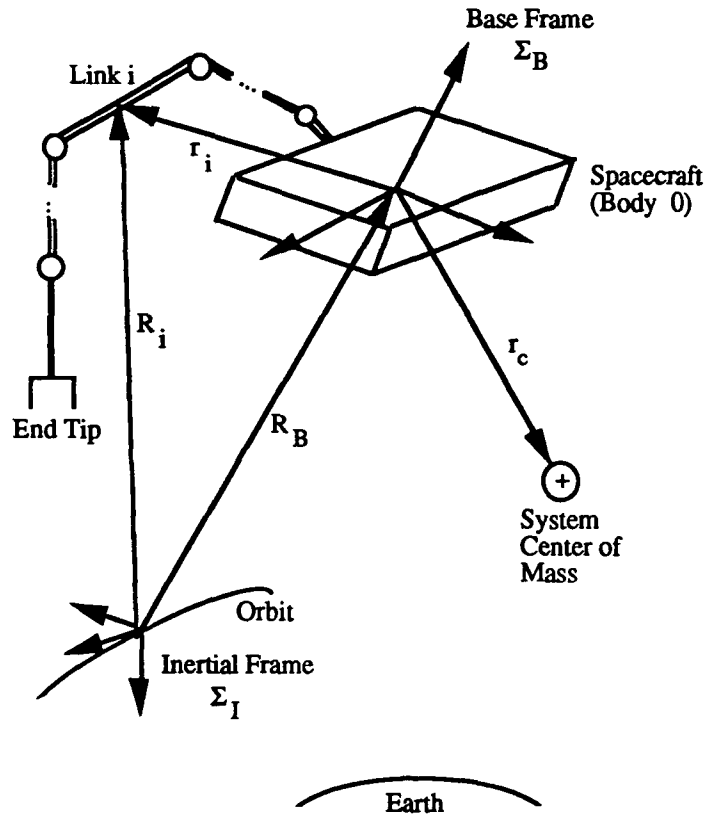


Figure 1. A Space Robot.

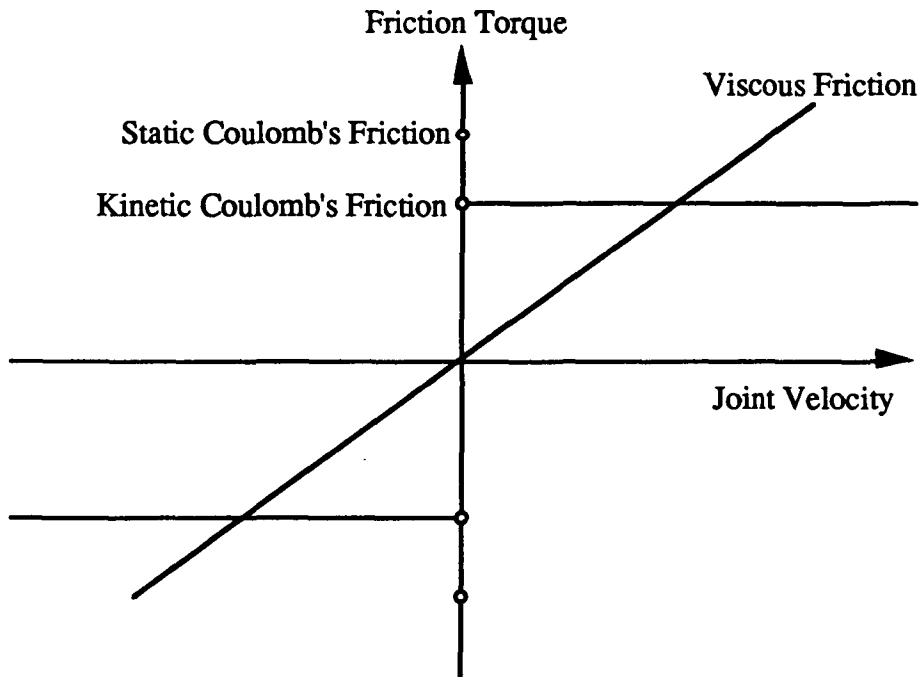


Figure 2. Friction Model Consisting of Coulomb's Friction and Linear Viscous Friction.

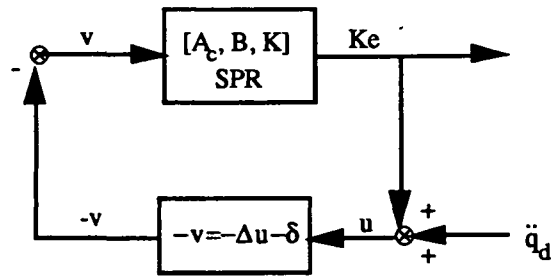


Figure 3. Robust Feedback Linearization Using Passivity Theorem.

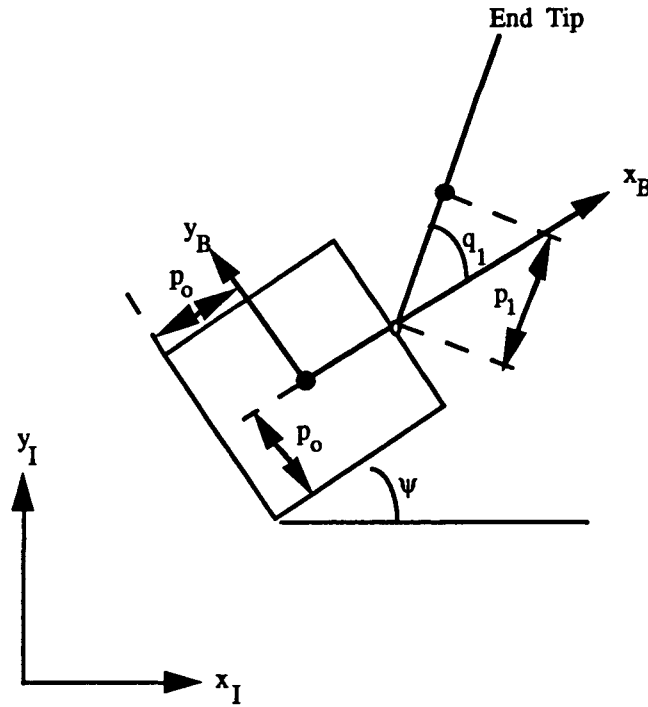


Figure 4. A Single Link Planar Space Robot.

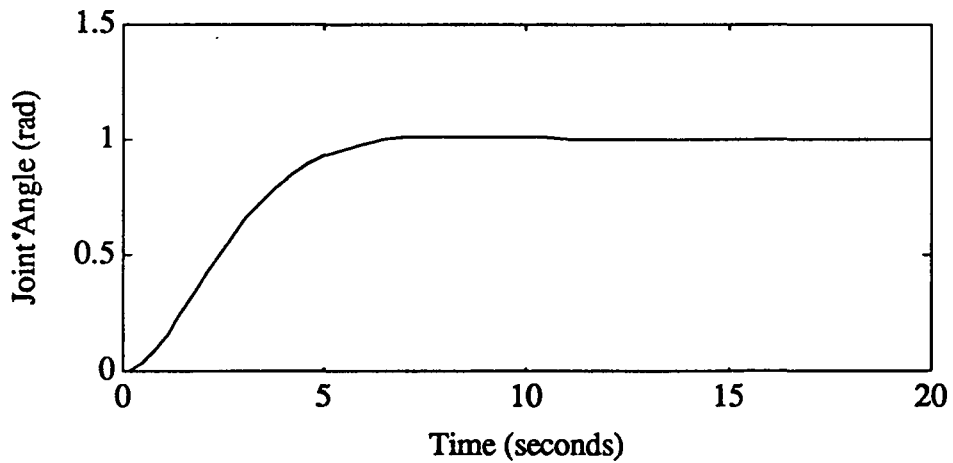


Figure 5. Joint Angle Response for the Single Link Planar Space Robot.

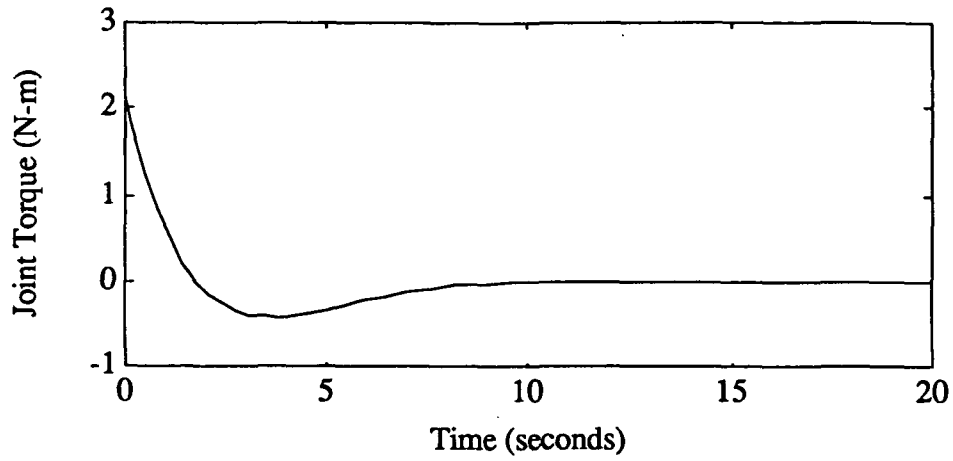


Figure 6. Joint Torque Input for the Single Link Planar Space Robot.

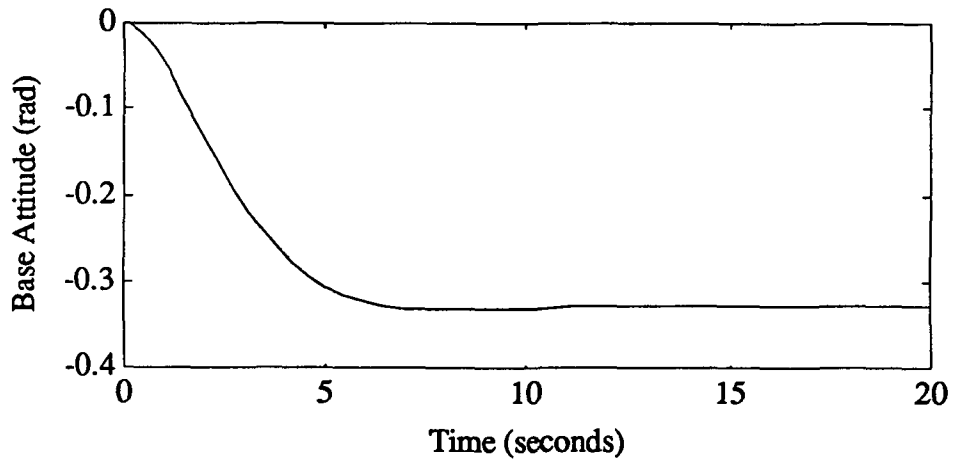


Figure 7. Base Attitude Response for the Single Link Planar Space Robot.

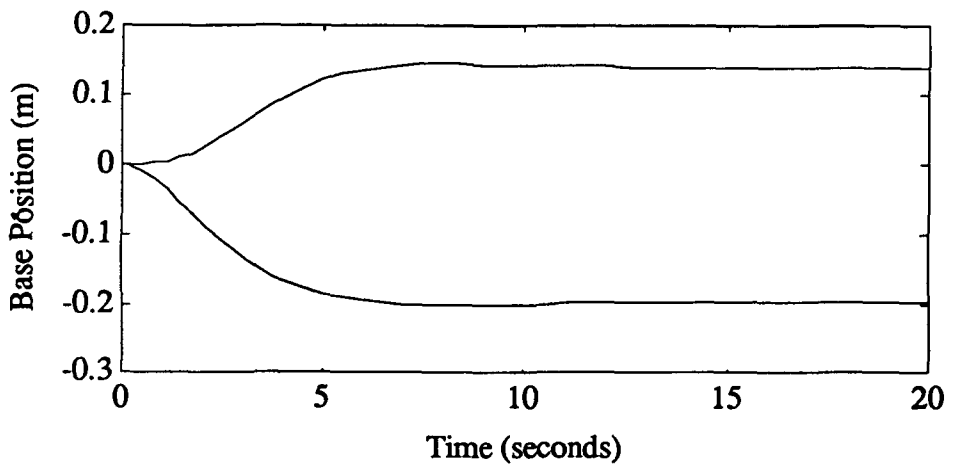


Figure 8. Motion of the Base Center of Mass for the Single Link Planar Space Robot.

Table I. Physical Parameters of Single Link Robot.

Body	p (meter)	l (meter)	m (kg)	I (kg.m ²)
0 (Base)	3.0	-	5.0	30.0
1 (Link)	3.0	6.0	1.0	3.0